



A ReaxFF Molecular Dynamics Study of Pyrolysis Mechanism of Normal and Isomeric Decanes

Yucheng Fan^{1,a}, Xiaoxiao Gong^{2,b}, Dongyuan Liu^{1,c}, Xiaohan Li^{1,d}, Xin Wang^{1,e},
Zhennan Liu^{1,f}, Houyu Zhu^{1,*}

¹School of Materials Science and Engineering, China University of Petroleum (East China),
Qingdao, Shandong, 266580, China

²State Key Laboratory of Molecular & Process Engineering, SINOPEC Research Institute of
Petroleum Processing Co., Ltd., Beijing, 10083, China

^afanyucheng2000@163.com, ^bgongxiaoxiao.ripp@sinopec.com

^cb21140013@s.upc.edu.cn, ^d444959738@qq.com

^e1250920215@qq.com, ^f215240556@qq.com

*hyzhu@upc.edu.cn

Abstract. Using the ReaxFF molecular dynamics method, we investigated the pyrolysis mechanisms of n-decane and its isomer (2-methyl-nonane) to assess how isomerization affects initial pyrolysis pathways and main product formation in straight-chain alkanes. The results indicate that at high temperatures, the initial pyrolysis pathways for both n-decane and 2-methyl-nonane primarily involve two routes, proceeding through C-C and C-H bond cleavages at different positions. Due to branched methyl groups, 2-methyl-nonane exhibits a more complex pyrolysis pathway, with a higher proportion of C-H bond cleavage compared to C-C bonds. Product analysis shows that the main products of n-decane pyrolysis are C₂H₄, CH₄, and H₂; after isomerization, the distribution changes, in which the C₂H₄ and H₂ peaks decrease but the CH₄ peak increases. Thus, branched methyl groups and shortened carbon chain notably affect the product distribution of n-decane. This study provides insights into the thermal decomposition characteristics of n-decane and 2-methyl-nonane at a molecular level, serving as a reference for further studies on isomerization effects of straight-chain alkanes as endothermic hydrocarbon fuel.

Keywords: Decane; Pyrolysis Mechanism; Isomerization; ReaxFF MD

1 Introduction

Supersonic aircraft is a cutting-edge technology in aerospace, operating under extreme high-temperature and high-speed conditions. During high-speed flights, temperatures in the combustion chamber and on the aircraft's surface rise sharply, causing significant damage to components and affecting normal operation. Heat-sink hydrocarbon fuels, as a class of high-performance combustible coolants, effectively address cooling and thermal management issues^[1]. The essence of this cooling process is that before

entering the combustion chamber, these fuels absorb heat through their heat capacity, phase transitions, and chemical cracking reactions, generating small molecular products with excellent combustion properties and energy density, such as ethylene and methane.

Hydrocarbon fuels with heat-absorbing properties are typically mixtures of various paraffins and naphthenes, making it challenging to directly study the thermal cracking mechanism of the original fuel. Therefore, representative components are often selected as research subjects. N-Decane is a key representative of paraffins in aviation fuel and plays an important role in developing alternative models for aviation fuel^[2]. In previous research, Zamosny et al.^[3] conducted pyrolysis studies on C1-C12 hydrocarbons using experimental methods and compared the pyrolysis products of straight-chain and branched-chain alkanes. However, a detailed analysis of the cracking mechanism was not undertaken. Currently, theoretical computational simulation has become an essential and powerful scientific research tool. The ReaxFF molecular dynamics method is widely used in the study of biomass, coal, and hydrocarbon fuel pyrolysis^{[4][5][6]}. Zhou et al.^[7] studied the pyrolysis of n-decane under varying electric field intensities using the ReaxFF molecular dynamics method, providing insights into its pyrolysis mechanism. However, research on the impact of structural changes during n-decane pyrolysis is lacking. Recently, Wang et al.^[8] studied the pyrolysis mechanisms of spiro[4,5]-decane (C₁₀H₁₈) and spiro[5,6]-dodecane (C₁₂H₂₂) using the ReaxFF molecular dynamics method, revealing how different carbocyclic structures and size effects influence the fuels' initial decomposition reactivity and product formation. The results show that the initial decomposition pathways for both spirocycloalkanes are similar, while chain alkanes and cycloalkenes exhibit distinct structural differences. Currently, there is limited research on the impact of isomerization on the pyrolysis behavior of n-decane. In this work, n-decane and its isomer 2-methyl-nonane were chosen as the model molecules to investigate how isomerization via methylation affects the pyrolysis mechanism of n-decane and influences the generation of main products, thereby providing a theoretical basis for understanding the pyrolysis characteristics of normal and isomeric alkanes as endothermic hydrocarbon fuel.

2 Simulation Method

Both systems employed the Amorphous Cell module in Materials Studio^[9] to create a three-dimensional periodic model with 50 molecules, initially set at a density of 0.1 g/cm³. Dynamic simulations were performed using the Forcite module under NVT and NPT ensembles for structural optimization. Models with densities of 0.23 g/cm³ for n-decane and 0.48 g/cm³ for 2-methyl-nonane were obtained, as shown in Fig. 1. The selected force field was Compass II with medium precision. The optimized models were exported from Materials Studio, and thermal decomposition was simulated using LAMMPS^[10] software, utilizing a reaction force field file containing C, H, and O elements^[11]. Simulations ran for 400 ps at 3000 K under the NVT ensemble, with a time step of 0.1 fs and trajectory data output every 1 ps. The reaction pathways during thermal decomposition were analyzed using ReacNetGenerator^[12], while product analysis was conducted via a Python program.

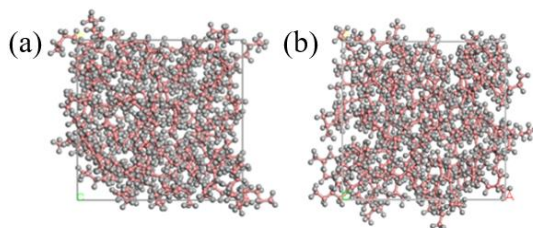


Fig. 1. Thermal decomposition simulation system of n-decane (a) and 2-methyl-nonane (b).

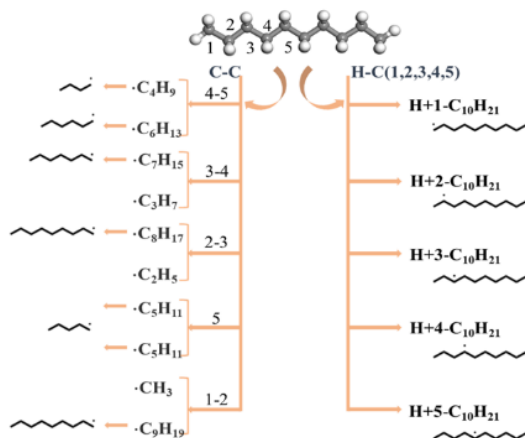


Fig. 2. The initial thermal decomposition reaction path of n-decane.

3 Results and Discussion

3.1 Initial Pyrolytic Reaction

The MD simulation results show that the initial pyrolysis of n-decane primarily begins with the cleavage of C-C and C-H bonds at various positions, as illustrated in Fig.2. Due to the symmetry of n-decane, only atoms C1 to C5 are labeled to indicate different bond cleavage positions. The decomposition involves 10 pyrolytic homolytic reactions, including 5 types of C-C bond cleavages: C1-C2, C2-C3, C3-C4, C4-C5, and a symmetrical cleavage in the middle of n-decane. This process generates a total of 9 small molecular radicals. Additionally, there are 5 types of C-H bond cleavages resulting from dehydrogenation at different carbon positions to form H atom radicals and five distinct C₁₀H₂₁ radicals. Analysis of the initial reaction frequencies, as shown in Fig.3, reveals that C-C bond cleavage accounts for 59% of the initial pyrolysis reaction, while C-H bond cleavage accounts for 41%, indicating a predominance of C-C bond cleavage. Among the C-C bond cleavages, the most susceptible position is the C4-C5 bond at 26%, followed by the C2-C3 and C3-C4 bonds. The least frequently cleaved position is the middle symmetrical break at only 12%. In terms of C-H bond cleavages, the H

atom at terminal position C1 is most readily cleaved, accounting for 32%, followed by positions C3 and C4. Dehydrogenation reactions at positions C2 and C5 are more challenging, with a proportion of 15%.

The initial pyrolysis of 2-methyl-nonane involves 17 pathways, including 8 C-C and 9 C-H bond cleavages. As shown in Fig.4, compared to n-decane, 2-methyl-nonane has a more complex cracking mechanism due to branched methyl groups in its structure. Additionally, C-C bond cleavages at various positions yield isomeric products. The radicals generated from the cleavage of the C3-C4 and C5-C6 bonds include both C_4H_9 and C_6H_{13} . We distinguish these isomers; for instance, the cleavage of the C3-C4 bond produces both the 2-methyl-propane radical and hexane radical. The products within the dashed box in Fig.4 represent a specific combination resulting from these processes. As shown in Fig.5, the proportion of C-H bond cleavage in 2-methyl-nonane is 52%, slightly higher than that of C-C bond cleavage.

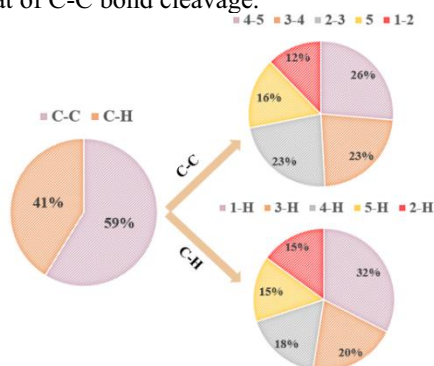


Fig. 3. The proportion of each initial thermal decomposition reaction path of n-decane.

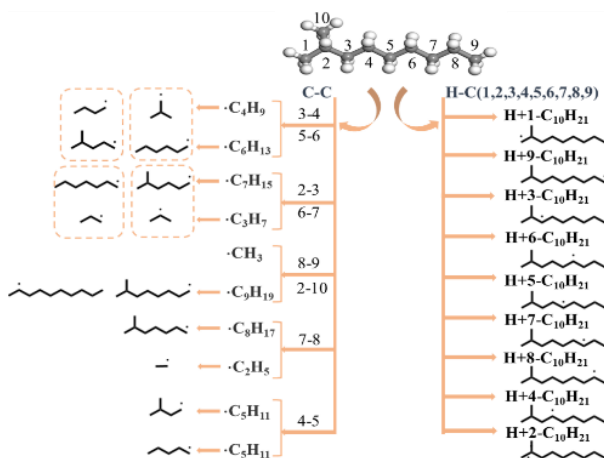


Fig. 4. The initial pyrolysis reaction route of 2-methyl-nonane.

In C-C bond cleavage reactions, the most susceptible position is the C3-C4 bond, accounting for 21%, while the most difficult position to rupture is the C2-C3 bond at

only 5%. For C-H bond cleavages, the most readily cleaved position is the dehydrogenation of the C1 atom adjacent to a methyl group, representing 29% (the H atoms at positions C1 and C10 have equivalent effects structurally; thus, the proportion of 1-H reflects both dehydrogenation reactions). The hardest dehydrogenation occurs at position C2, which accounts for just 2%. Clearly, branched methyl groups significantly influence C-C bond cleavage during n-decane's initial pyrolysis reaction, shifting the easiest cleaved position from C4-C5 to C3-C4.

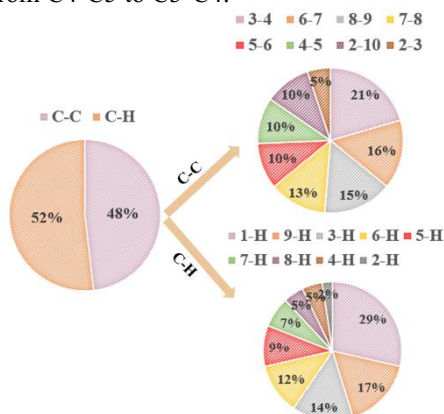


Fig. 5. The proportion of each initial pyrolysis reaction path of 2-methyl-nonane.

3.2 The Variations of the Principal Products with Time and the Impact of Isomerization on the Products

Fig.6(a) illustrates the temporal trends of the products derived from n-decane. In this analysis, only the five predominant products with the highest yields in n-decane were considered: ethylene (C_2H_4), methane (CH_4), hydrogen (H_2), acetylene (C_2H_2), and propyne (C_3H_4). The blue lines in Fig.6(a) and 6(b) represent the temporal variations in quantities for both n-decane and 2-methyl-nonane, respectively. It is evident that upon initiation of the pyrolysis reaction, n-decane undergoes rapid cracking, achieving complete decomposition at approximately 50 ps. In contrast, 2-methyl-nonane is predominantly cracked around 20 ps, with a negligible amount remaining until it fully decomposes by about 70 ps. Thus, the presence of branched methyl groups significantly reduces the cracking time of n-decane. Regarding product distribution as depicted in Fig.6(a), due to its relatively swift initial cracking reaction, C_2H_4 , CH_4 , and H_2 exhibit rapid increases within the first 100 ps; notably, C_2H_4 shows a particularly pronounced increase. Following their peak values, both C_2H_4 and CH_4 experience slight but steady declines while H_2 continues to rise consistently. Conversely, C_2H_2 and C_3H_4 display an overall slow growth trend. As illustrated in Fig.6(b), although being an isomer of n-decane, the trends for major products from 2-methyl-nonane are similar; however, there are significant differences in their respective quantities. Notably excluding CH_4 from this observation reveals that other primary products show markedly lower yields overall. Consequently, it can be inferred that branched methyl groups along with shortened carbon chains facilitate increased production of CH_4 while concurrently diminishing

yields of other principal products. The preceding analysis clearly shows that C_2H_4 , CH_4 , and H_2 have the highest proportions among the products. To further investigate their formation mechanisms, the ReacNetGenerator program was used to analyze kinetic simulation trajectories and statistically determine the generation paths of these products. The results indicate that C_2H_4 is primarily formed through beta-bond cleavage reactions involving various free radicals (such as 1-hexyl, 1-heptyl, and 1-octyl) from initial cracking; CH_4 mainly arises from the combination of methyl free radicals with H free radicals produced during cracking; H_2 is predominantly generated by combining H free radicals resulting from cracking.

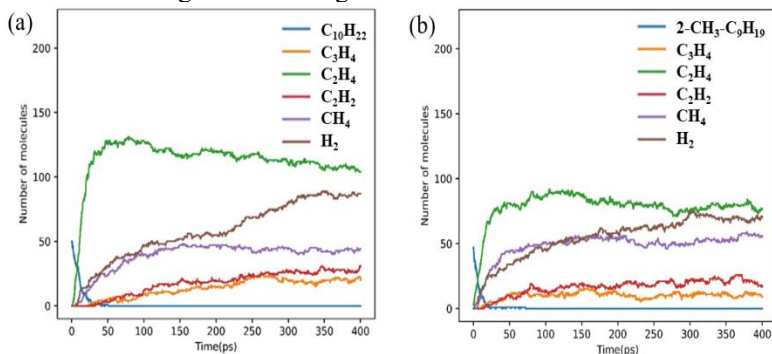


Fig. 6. The variations of the major products of n-decane (a) and 2-methyl-nonane (b) with time.

4 Conclusion

(1) The initial pyrolysis reactions of both n-decane and 2-methylnonane are initiated by the cleavage of C-C and C-H bonds. The reaction pathways for isomerized 2-methylnonane are more complex, resulting in the simultaneous formation of isomers among the products. The presence of branched methyl groups significantly influences the reactivity of C-C bonds in n-decane at elevated temperatures, with the most readily cleaved bond position shifting from C4-C5 to C3-C4. In contrast, the effect on C-H bonds remains minimal, with the carbon atom most susceptible to dehydrogenation being located at position C1.

(2) The principal products of n-decane pyrolysis include five species: C_2H_4 , CH_4 , H_2 , C_2H_2 , and C_3H_4 . Throughout the kinetic simulation process, the quantities of C_2H_4 , CH_4 , and H_2 exhibit the most pronounced variations. Isomerization significantly influences the distribution of main products. The presence of branched methyl groups and the shortening of carbon chains promote the formation of CH_4 while concurrently diminishing the yields of other primary products.

Acknowledgement

Supported by State Key Laboratory of Molecular & Process Engineering (RIPP, SINOPEC) (36800000-23-ZC0699-0042) and the National Natural Science Foundation of China (22072182).

References

1. Liu C, Qiu S Y, Huang H M, et al. Mechanism of Thermal Decomposition of Endothermic Hydrocarbon Fuel n-Octane[J]. *Materials Reports*, 2019, 33(8): 1251-1256. <https://doi.org/10.11896/cldb.18040185>.
2. Yu Y, Song L, Jiang J, et al. Reactive molecular dynamics simulations of multicomponent models for RP-3 jet fuel in combustion at supercritical conditions: A comprehensive mechanism study[J]. *Chemical Physics*, 2023, 573: 112008. <https://doi.org/10.1016/j.chemphys.2023.112008>.
3. Zámostný P, Bělohav Z, Starkbaumová L, et al. Experimental study of hydrocarbon structure effects on the composition of its pyrolysis products[J]. *Journal of Analytical and Applied Pyrolysis*, 2010, 87(2): 207-216. <https://doi.org/10.1016/j.jaap.2009.12.006>.
4. Lele A, Kwon H, Ganeshan K, et al. ReaxFF molecular dynamics study on pyrolysis of bicyclic compounds for aviation fuel[J]. *Fuel*, 2021, 297: 120724. <https://doi.org/10.1016/j.fuel.2021.120724>.
5. Zhang X, Lu X, Xiao M, et al. Molecular reaction dynamics simulation of pyrolysis mechanism of typical bituminous coal via ReaxFF[J]. *Journal of Fuel Chemistry and Technology*, 2020, 48(9): 1035-1046. [https://doi.org/10.1016/S1872-5813\(20\)30071-2](https://doi.org/10.1016/S1872-5813(20)30071-2).
6. Liu Y, Zhong Z, Xu S. Pyrolysis mechanism of tetrahydrotricyclopentadiene by ReaxFF reactive molecular dynamics simulations[J]. *Computational and Theoretical Chemistry*, 2022, 1213: 113735. <https://doi.org/10.1016/j.comptc.2022.113735>.
7. Zhou W, Zhang X, Zhou W, et al. Inhibition mechanism of electric field on polycyclic aromatic hydrocarbon formation during n-decane pyrolysis: A ReaxFF MD and DFT study[J]. *Journal of the Energy Institute*, 2022, 102: 82-91. <https://doi.org/10.1016/j.joei.2022.02.013>.
8. Wang H, Sun X, Zhou Y, et al. Study on pyrolysis mechanism and kinetics of spiro 4, 5 decane and spiro 5, 6 dodecane[J]. *Journal of Fuel Chemistry and Technology*, 2024, 52(7): 1020-1034. <https://doi.org/10.19906/j.cnki.JFCT.2024001>.
9. B. Delley. From molecules to solids with the DMol 3 approach[J]. *The Journal of chemical physics*, 2000, 113(18): 7756-7764.
10. Chenoweth K, Van Duin A C T, Goddard W A, et al. ReaxFF reactive force field for molecular dynamics simulations of hydrocarbon oxidation[J]. *The Journal of Physical Chemistry A*, 2008, 112(5): 1040-1053. <https://doi.org/10.1021/jp709896w>.
11. Cheng X M, Wang Q D, Li J Q, et al. ReaxFF molecular dynamics simulations of oxidation of toluene at high temperatures[J]. *The Journal of Physical Chemistry A*, 2012, 116(40): 9811-9818. <https://doi.org/10.1021/jp304040q>.
12. Zeng J, Cao L, Chin C H, et al. ReacNetGenerator: an automatic reaction network generator for reactive molecular dynamics simulations[J]. *Physical Chemistry Chemical Physics*, 2020, 22(2): 683-691. <https://doi.org/10.1039/C9CP05091D>.

Open Access This chapter is licensed under the terms of the Creative Commons Attribution-NonCommercial 4.0 International License (<http://creativecommons.org/licenses/by-nc/4.0/>), which permits any noncommercial use, sharing, adaptation, distribution and reproduction in any medium or format, as long as you give appropriate credit to the original author(s) and the source, provide a link to the Creative Commons license and indicate if changes were made.

The images or other third party material in this chapter are included in the chapter's Creative Commons license, unless indicated otherwise in a credit line to the material. If material is not included in the chapter's Creative Commons license and your intended use is not permitted by statutory regulation or exceeds the permitted use, you will need to obtain permission directly from the copyright holder.

